

X. ZHANG^{1,2}
G. BERGER^{1,✉}
M. DIETZ¹
C. DENZ¹

Cross-talk in phase encoded volume holographic memories employing unitary matrices

¹ Institut für Angewandte Physik, Westfälische Wilhelms-Universität Münster, Corrensstr. 2–4, 48149 Münster, Germany

² TEDA Applied Physics School, Nankai University, 300457 Tianjin, P.R. China

Received: 3 April 2006/Revised version: 20 July 2006
Published online: 8 September 2006 • © Springer-Verlag 2006

ABSTRACT The cross-talk noise in phase encoded holographic memories employing unitary matrices is theoretically investigated. After reviewing some earlier work in this area, we derive a relationship for the noise-to-signal ratio for phase-code multiplexing with unitary matrices. The noise-to-signal ratio rises in a zigzag way on increasing the storage capacity. Cross-talk is mainly caused by high-frequency phase codes. Unitary matrices of even orders have only one bad code, while unitary matrices of odd orders have four bad codes. The signal-to-noise ratios of all other codes can in each case be drastically improved by omission of these bad codes. We summarize the optimal orders of Hadamard and unitary matrices for recording a given number of holograms. The unitary matrices can enable us to adjust the available spatial light modulators to achieve the maximum possible storage capacity in both circumstances with and without bad codes.

PACS 42.40.Lx; 42.40.Ht; 42.40.Pa

1 Introduction

Volume holographic memories offer high storage capacities and short data access times through multiplexing and a page-oriented storage principle [1]. Multiple holograms can be recorded in the storage media through various multiplexing techniques, such as angular, phase-code, wavelength or shift multiplexing [2–5]. Among the different methods, deterministic phase-code multiplexing has been widely investigated since it entails several advantages [6–13]. This method uses a fixed wavelength and geometry without introducing mechanically moving parts [6]. Orthogonal phase-code multiplexing allows us to perform parallel optical addition, subtraction, and inversion operations of stored images [8]. Moreover, associative recall, relying on simple intensity measurements has been realized [10, 11].

Typically Walsh–Hadamard matrices (H matrices) are employed in order to generate orthogonal phase codes. The traditional H matrices, whose orders are a power of 2, can be easily generated by means of the Kronecker product. Algorithms for constructing general H matrices, whose orders are equal to $4m$

(with m a positive integer), have been thoroughly discussed by Yang et al. [12] Recently, unitary matrices (U matrices) have been proposed, which can be utilized in order to generate unitary phase codes for phase-code multiplexing [13]. U matrices can be easily constructed with geometric sequences, whose orders can be any positive integer.

The storage capacity is determined by the signal-to-noise ratio (SNR) of the retrieved data. Cross-talk noise due to diffraction from non-Bragg-matched gratings is involved in estimating the SNRs [14–20]. Gu et al. [14] discussed cross-talk in Fourier hologram systems which are based on angular multiplexing. Curtis et al. adapted this method to investigate memories based on wavelength multiplexing [15] and phase-code multiplexing utilizing H matrices [16]. Cross-talk in phase encoded systems is mainly caused by high-frequency codes, which are so-called bad codes. The overall SNRs can be significantly improved by omitting these bad codes [16]. The general H matrix for a given order is usually not unique. Different H matrices result in different SNR distributions and specific bad codes cannot be identified [18]. A brief analysis shows that the SNRs in phase-encoded memories utilizing traditional H matrices and U matrices are of the same order of magnitude if both matrices have the same order 64 [13]. Here we present detailed analysis of cross-talk noise for phase-code multiplexing with U matrices. At first we review earlier methods [14, 16] to derive an expression for the noise-to-signal ratio (NSR) for phase-code multiplexing employing U matrices. Subsequently we discuss the SNR characteristics and identify bad codes of U matrices of even and odd orders. Finally, we summarize the optimal orders of matrices to a given number of holograms for different situations in phase-coded holographic memories.

2 Theory

A hologram is the recording of an optical interference pattern, which is formed at the intersection of two coherent optical beams, the signal and reference beams. The signal beam is usually modulated by a spatial light modulator (SLM) that represents data as a two-dimensional (2-D) bit pattern $f(x_0, y_0)$, as shown in Fig. 1. The SLM is placed in the input plane, i.e. the front focal plane of lens L_1 . This lens yields the Fourier transform of the input signal in its rear focal plane (x, y, z) , in which the recording medium is placed.

✉ Fax: +49-251-83-33513, E-mail: gberger@uni-muenster.de

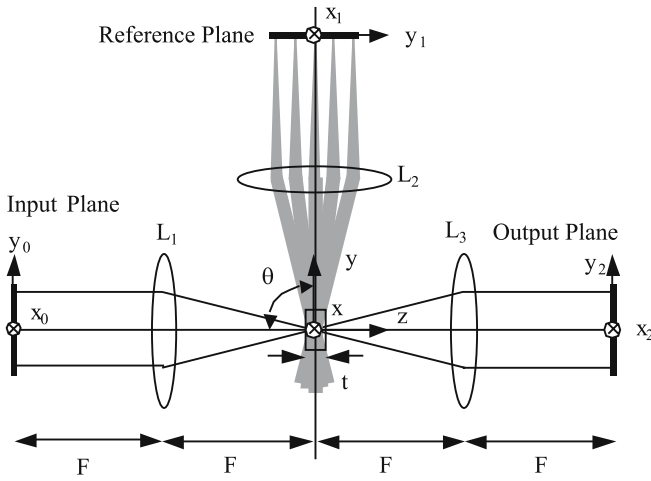


FIGURE 1 Recording and readout geometry for phase-code multiplexing

In systems based on angular multiplexing the reference beam is typically a plane wave, whose angle of incidence is controlled in order to superimpose many holograms. In systems based on phase-code multiplexing the reference beam consists of many plane waves, whose phases are modulated by means of a phase spatial light modulator (PSLM). The set of phases used to record one data page, called the phase code, represents its storage address.

2.1 Diffraction from a volume hologram

When recording a Fourier-transform hologram by a signal beam S and a reference beam R , the resultant change of the permittivity of the storage medium can be written as

$$\Delta\varepsilon \approx R^*S + \text{c.c.}, \quad (1)$$

in which c.c. represents the complex conjugate. We use a $\theta = 90^\circ$ configuration in our storage system, for the maximum number of data pages that can be stored by using this configuration [14]. The reference beam is a simple plane wave

$$R = \exp(j\mathbf{k}_r \cdot \mathbf{r}), \quad (2)$$

where \mathbf{k}_r is the wave vector determined by the position of the reference point at the front focal plane of the lens L_2 . Under the paraxial approximation, the wave vector is given by

$$\mathbf{k}_r = \left(0, \frac{y_r^2}{2F^2} - 1, -\frac{y_r}{F} \right) \mathbf{k}, \quad (3)$$

where F is the focal length of the lenses L_1 , L_2 , and L_3 (cf. Fig. 1), \mathbf{k} is given as $2\pi/\lambda$ and λ is the wavelength of the recording beams. Based on standard Fourier-optics analysis [14, 16, 21], the signal beam is given by

$$S(\mathbf{r}) \approx \exp(jkz) \iint dx_0 dy_0 f(x_0, y_0) \times \exp \left[-j\frac{k}{F}(xx_0 + yy_0) \right] \exp \left[-j\frac{kz}{2F^2}(x_0^2 + y_0^2) \right]. \quad (4)$$

During readout the recorded holograms are probed by a plane wave with wave vector \mathbf{k}_p . According to the scalar diffraction theory [14, 16, 22], the outgoing electric field can be written as

$$E(\mathbf{k}_d) \approx \int d\mathbf{r}' \Delta\varepsilon(\mathbf{r}') \exp(-j\mathbf{K} \cdot \mathbf{r}'), \quad (5)$$

where $\mathbf{K} = \mathbf{k}_d - \mathbf{k}_p$, \mathbf{k}_d is the wave vector of the diffracted plane-wave component. Each diffracted plane-wave component is converted to a point at the rear focal plane of the lens L_3 . Under the paraxial approximation the relationship between the wave vector and the coordinates of the point is given by [14]

$$\mathbf{k}_d = \left(\frac{x_2}{F}, \frac{y_2}{F}, 1 - \frac{x_2^2}{2F^2} - \frac{y_2^2}{2F^2} \right) \mathbf{k}. \quad (6)$$

By using (1)–(4) and (6), the integral in (5) can be evaluated. When assuming that the transverse dimensions of the medium are large enough to record all spatial frequency components of the signal waves and $y_r, y_p \ll F$, the electric field at the output plane can be written as

$$E(x_2, y_2) \approx f(-x_2, -y_2) \times \text{sinc} \left\{ \frac{t}{\lambda F} \left[(y_p - y_r) + \frac{(y_r^2 - y_p^2)}{2F^2} y_2 \right] \right\}, \quad (7)$$

where t is the thickness of the storage medium, i.e. the holograms thickness. Considering only the central ray of the signal beam, i.e. $y_2 = 0$, (7) can be rewritten in a simplified form as

$$E(x_2, y_2) \approx f(-x_2, -y_2) \text{sinc} \left[\frac{t}{\lambda F} (y_p - y_r) \right]. \quad (8)$$

Maximum diffraction efficiency is achieved for $y_p = y_r$, which is called Bragg matching. When the sinc function reaches its first null, $\Delta = y_p - y_r = \lambda F/t$, which is called the Bragg selectivity.

2.2 Cross-talk of angular multiplexing

Suppose that two holograms are recorded with the same signal beam and two different plane reference beams, which are separated by Δ at the reference plane. If the holograms are illuminated by one of the reference beams, according to (8) only the corresponding signal wave is reconstructed, i.e. there is no contribution from the other hologram. As a result more holograms can be superimposed in the same volume if all adjacent reference points are separated by Δ , which is the principle of angular multiplexing.

In practice the signal is a 2-D data page, the diffraction from the other hologram will not be zero when $y_2 \neq 0$. If one hologram is recorded with $y_r = 0$ and the second hologram with $y_r = (1 + \delta)\Delta$, where $|\delta| \ll 1$, a probe beam from reference point $y_p = (1 + \delta)\Delta$ reconstructs the second hologram. Based on (7) the NSR of the second hologram can be calculated as

$$\text{NSR} = \text{sinc}^2 \left[(1 + \delta) - \frac{\lambda(1 + \delta)^2}{2Ft} y_2 \right]. \quad (9)$$

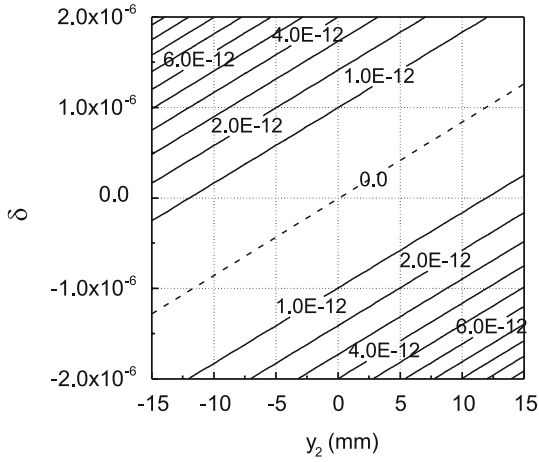


FIGURE 2 Contour plot of NSR as a function of both the location of the output plane y_2 and the location of the reference plane δ

The δ vs. y_2 diagram in Fig. 2 shows the contour lines of the NSR for the same parameters as used in [16] ($t = 10$ mm, $\lambda = 500$ nm, $F = 300$ mm, and $y_{2\max} = 15$ mm). There is a noise-free line, but it is not possible to achieve noise-free reconstruction for all points at the output plane. If $\delta = 0$, the maximum NSR occurs at $y_{2\max}$. In order to evaluate the worst-case NSR, y_2 is set to $y_{2\max}$, which results in the maximum NSR (for $\delta = 0$).

Suppose now N holograms are multiplexed by separating adjacent reference points by Δ . Then the worst-case NSR of the m th hologram is given by

$$\text{NSR} = \sum_{l \neq m, l=-M}^M \text{sinc}^2 \left[(m-l) + \frac{\lambda y_{2\max}}{2Ft} (l^2 - m^2) \right], \quad (10)$$

where $M = (N-1)/2$ and $m = -M, -M+1, \dots, M-1, M$. Note that the indices of the holograms span from $-M$ to M (which is a different notation as used in [13]).

2.3 Cross-talk of phase-code multiplexing

In phase-code multiplexing each reference beam consists of a set of plane waves, whose phases are modulated by a PSLM. For storing N holograms, N phase codes are utilized. The m th hologram is recorded by interfering the signal beam S_m with the reference beam R_m in the storage media. The complex amplitude of the m th reference beam with the l th component being phase modulated by U_{ml} can be written as

$$R_m = \sum_{l=-M}^M U_{ml} \exp(jk_l \cdot \mathbf{r}). \quad (11)$$

The entries of the U matrices are given by

$$U_{ml} = \exp \left[j \frac{2\pi(m+M)(l+M)}{N} \right], \quad (12)$$

where the indices are not integers if the orders of the corresponding U matrices are even.

If the holograms are illuminated with the n th reference beam, the electric field at the output plane can be written as

$$E(x_2, y_2) \approx \sum_{m=-M}^M \left| \sum_{k=-M}^M \sum_{l=-M}^M U_{n,k} U_{m,l}^* f_m(-x_2, -y_2) \right. \\ \left. \times \text{sinc} \left[(k-l) + \frac{\lambda y_2}{2Ft} (l^2 - k^2) \right] \right|. \quad (13)$$

Assuming a random distribution of the ON bits over each page and taking into account the unitarity of phase codes [13], the NSR of the n th hologram is given by

$$\text{NSR} = \frac{1}{N^2} \sum_{m \neq n, m=-M}^M \left| \sum_{k=-M}^M \sum_{l \neq n, l=-M}^M U_{n,k} U_{m,l}^* \right. \\ \left. \times \text{sinc} \left[(k-l) + \frac{\lambda y_2}{2Ft} (l^2 - k^2) \right] \right|^2. \quad (14)$$

3 Calculation and discussion

Figure 3 shows a plot of the NSR as a function of both the location of the output plane y_2 and the number of holograms N with the code number $n = -M$. The worst-case NSR occurs at $y_{2\max}$, the edge of the output plane. The worst-case NSR rises in a zigzag manner when increasing the storage capacity, i.e. the worst-case NSR of $N+2$ holograms is larger than that of N holograms and the worst-case NSR of $2N+1$ holograms is smaller than that of $2N$ holograms.

According to (14) the SNRs of phase-code members R_n and R_{1-n} are equal, e.g. the SNRs of $R_{-0.5}$ and $R_{0.5}$ in the set U^{100} or the SNRs of R_0 and R_1 in the set U^{101} . Figure 4 shows the worst-case SNR versus the phase-code number n for U^{100} and U^{101} by setting y to its maximum value. The SNRs for U^{101} are better than those for U^{100} , which agrees

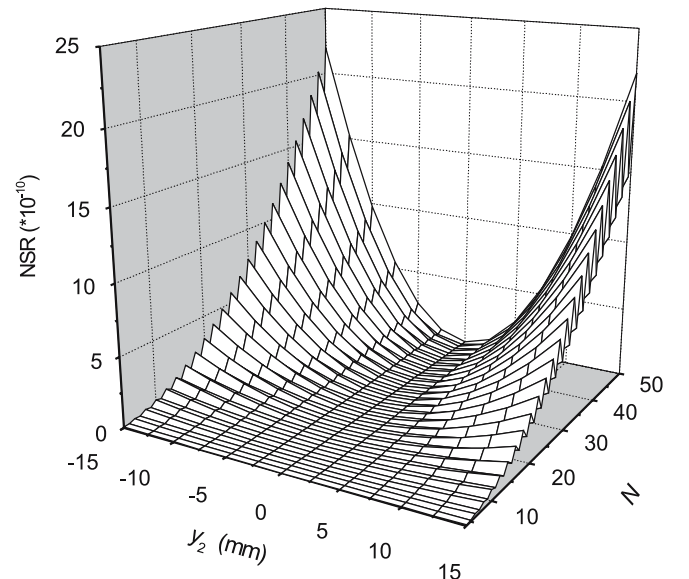


FIGURE 3 NSR as a function of both the location of the output plane y_2 and the total number of holograms N

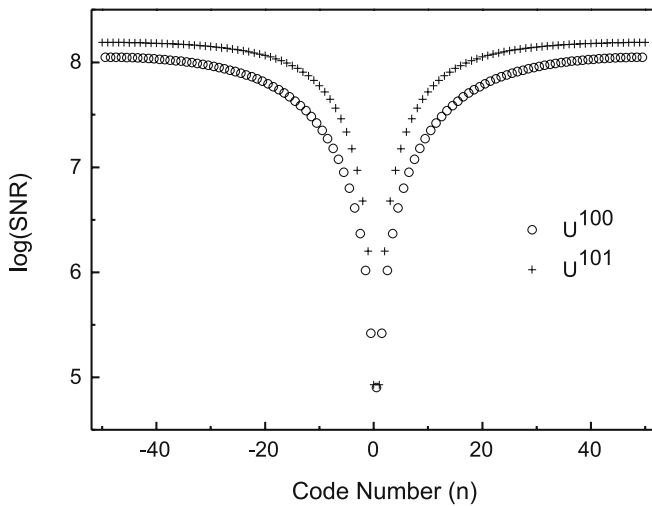


FIGURE 4 Worst-case log(SNR) versus hologram code number n

with the result shown in Fig. 3. The center code has the lowest SNR since it possesses the highest spatial frequency. The worst-case SNRs take place at code number $n = 0.5$ for U matrices of even orders and at $n = 0$ (and 1) for U matrices of odd orders, respectively. These high-frequency phase codes are the dominant noise source in terms of the present theoretical analysis. However by omitting the codes R_{-1} , R_0 , R_1 , and R_2 when utilizing U matrices of odd orders, the overall SNRs can be significantly improved. On the other hand, if U matrices of even orders are employed, the code $R_{0.5}$ should be omitted. That is, at the expense of slightly less storage capacity, the SNR performance can be drastically improved, as shown in Fig. 5.

Figure 6 compares the worst-case SNR of angular multiplexing and phase-code multiplexing utilizing U matrices. The worst-case SNR of phase-code multiplexing without the bad codes occurs when $n = -M$, while the worst-case SNRs with the bad codes occur when $n = 0.5$ for even N and $n = 0$ for odd N , respectively. When increasing N , the SNR of phase-code multiplexing including the bad codes drops faster than that of angular multiplexing. By omitting the bad codes, the SNR of phase-code multiplexing decreases much slower. For example, if $N = 960$, $\log(\text{SNR})$ is equal to 0.98, 3.39, and 6.32 for phase-code multiplexing including the bad codes, angular multiplexing, and phase-code multiplexing without the bad codes, respectively.

Hence for any given number of holograms N' that are to be stored, it is desirable to point out the best phase-code matrix in terms of the SNR performance. If $N' = 2^{n-1} + 1$ holograms are to be stored by use of traditional H matrices, an H matrix of order $N = 2^n$ has to be chosen to generate the re-

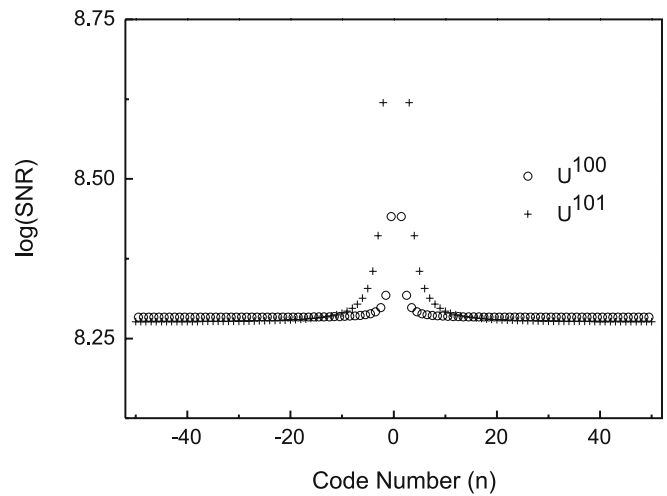


FIGURE 5 Worst-case log(SNR) versus hologram code number n without bad codes. U^{100} without code $R_{0.5}$; U^{101} without codes R_{-1} , R_0 , R_1 , and R_2

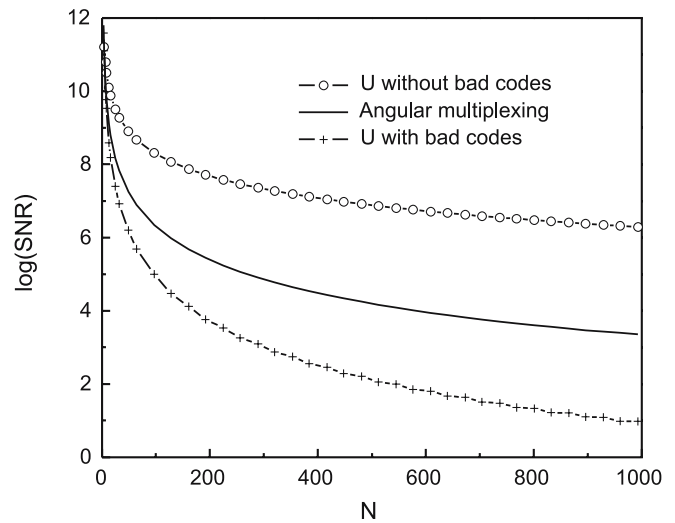


FIGURE 6 Worst-case log(SNR) versus the total number of holograms N for angular multiplexing and phase-code multiplexing utilizing U matrices

quired phase codes. Since there is a great difference between N' and N , one has to use a large enough PSLM to modulate all plane waves. As shown in Table 1, the general H matrices reduce this difference considerably, and the U matrices eliminate it. For instance, in order to store 257 holograms, the orders of the associated matrices will be 512, 260, and 257 for traditional H matrix, general H matrix, and U matrix, respectively. As we discussed above, the SNR can be greatly improved by omitting the bad codes. However, the general H matrices have no obvious bad code [18]. Therefore, if we want to improve the SNR of H Matrices, we should use the

	Type of matrices	N'	N	Reference
With bad codes	Traditional H matrices	$2^{n-1} + 1 \sim 2^n$	2^n	[3]
	General H matrices	$4n - 3 \sim 4n$	$4n$	[12]
	U matrices	n	n	[13]
Without bad codes	Traditional H matrices	$2^{n-1} \sim 2^n - 1$	2^n	[16]
	General H matrices	$2^{n-1} \sim 2^n - 1$	2^n	[18]
	U matrices	$2n - 2, 2n - 1$	$2n$	present study

TABLE 1 Summary of the optimal orders of matrices N' and the number of holograms N

traditional H matrices instead of general matrices. For example, H^{128} is the best choice to generate phase codes for storing 97 holograms. The maximum storage capacities will decrease slightly to $N - 4$ and $N - 1$ for U matrices with odd and even orders N , respectively. According to Fig. 6, the optimal order of U matrix is 98 rather than 101 for storing 97 holograms. Table 1 summarizes the different situations. Based on the present evaluation, one can use the smallest PSLM when utilizing unitary phase codes. In other words, U matrices enable us to achieve the maximum possible storage capacity for a given SLM configuration.

4 Conclusions

We have presented detailed cross-talk analysis of phase-code multiplexing utilizing U matrices. The NSR rises in a zigzag pattern as we increase the storage capacity. U matrices of even orders have only one bad code $R_{0.5}$, while U matrices of odd orders have four bad codes R_{-1} , R_0 , R_1 , and R_2 . The SNRs of all other codes will increase on omitting these bad codes. The SNRs of phase-code multiplexing utilizing U matrices and traditional H matrices are of the same order of magnitude. By taking out the code $R_{0.5}$, the average SNRs of U matrices, whose orders are even but not a power of 2, are higher than those of general H matrices. The optimal orders of Hadamard matrices and unitary matrices for storing a given number of holograms are summarized in Table 1. In both circumstances, with or without bad codes, U matrices ensure an optimal utilization of the available spatial light modulator in order to obtain the maximum possible storage capacity.

ACKNOWLEDGEMENTS We acknowledge the support from the Deutsche Forschungsgemeinschaft, the National Natural Science Foundation of China (Grant No. 60208003), and the Alexander von Humboldt Foundation.

REFERENCES

- 1 R. Shelby, J. Hoffnagle, G. Burr, C. Jefferson, M. Bernal, H. Coufal, R. Grygier, H. Günther, R. Macfarlane, G. Sincerbox, *Opt. Lett.* **22**, 1509 (1997)
- 2 L. d'Auria, J. Huignard, E. Spitz, *IEEE Trans. Magn.* **9**, 83 (1973)
- 3 C. Denz, G. Pauliat, G. Roosen, T. Tschudi, *Opt. Commun.* **85**, 171 (1991)
- 4 G. Rakuljic, V. Leyva, A. Yariv, *Opt. Lett.* **17**, 1471 (1992)
- 5 D. Psaltis, M. Levene, A. Pu, G. Barbastathis, K. Curtis, *Opt. Lett.* **20**, 782 (1995)
- 6 C. Denz, G. Pauliat, G. Roosen, T. Tschudi, *Appl. Opt.* **31**, 5700 (1992)
- 7 C. Alves, G. Pauliat, G. Roosen, *Opt. Lett.* **19**, 1894 (1994)
- 8 C. Denz, T. Dellwig, J. Lembcke, T. Tschudi, *Opt. Lett.* **21**, 278 (1996)
- 9 C. Denz, K.-O. Mueller, T. Heimann, T. Tschudi, *IEEE J. Sel. Top. Quantum Electron.* **4**, 832 (1998)
- 10 G. Berger, C. Denz, S.S. Orlov, B. Phillips, L. Hesselink, *Appl. Phys. B* **73**, 839 (2001)
- 11 G. Berger, M. Stumpe, M. Hoehne, C. Denz, *J. Opt. A* **7**, 567 (2005)
- 12 X. Yang, Y. Xu, Z. Wen, *Opt. Lett.* **21**, 1067 (1996)
- 13 X. Zhang, G. Berger, M. Dietz, C. Denz, *Opt. Lett.* **31**, 1047 (2006)
- 14 C. Gu, J. Hong, I. McMichael, R. Saxena, F. Mok, *J. Opt. Soc. Am. A* **9**, 1978 (1992)
- 15 K. Curtis, G. Gu, D. Psaltis, *Opt. Lett.* **18**, 1001 (1993)
- 16 K. Curtis, D. Psaltis, *J. Opt. Soc. Am. A* **10**, 2547 (1993)
- 17 M. Bashaw, J. Heanue, A. Aharoni, J. Walkup, L. Hesselink, *J. Opt. Soc. Am. B* **11**, 1820 (1994)
- 18 Z. Wen, Y. Tao, *Opt. Commun.* **148**, 11 (1998)
- 19 H. Lee, Y. Kim, D. Han, B. Lee, *J. Opt. Soc. Am. A* **16**, 563 (1999)
- 20 H. Kim, Y.H. Lee, *Opt. Lett.* **29**, 113 (2004)
- 21 J.W. Goodman, *Introduction to Fourier Optics* (McGraw-Hill, New York, 1968)
- 22 J.D. Jackson, *Classical Electrodynamics* (Wiley, New York, 1975)